J Seismol
DOI 10.1007/s10950-012-9288-5

ORIGINAL ARTICLE

Examining ambient noise using colocated measurements of rotational and translational motion

Celine Hadziioannou · Peter Gaebler · Ulrich Schreiber · Joachim Wassermann · Heiner Igel

Received: 21 October 2011 / Accepted: 16 February 2012

Abstract In the past decade, a number of studies have reported the observation of rotational motion associated with seismic events. We report a first observation of rotational motion in the microseismic ambient noise band. A striking feature of rotational motion measurements is that the information about the seismic phase velocity and source back azimuth is contained in the amplitude ratio of a point measurement of rotation rate and transverse acceleration. We investigate the possibility of applying this method to ambient noise measured with a ring laser and a broadband seismometer at the Wettzell Geodetic Observatory in Germany. Using data in the secondary microseismic band, we recover local phase velocities as well as the back azimuth of the strongest noise source for two different time periods. In order to confirm these findings, we additionally compare the results with classical array processing techniques of the Gräfenberg array located nearby.

Keywords Rotational ground motion · Ring laser · Ambient noise

C. Hadziioannou (✉) · H. Igel · J. Wassermann
Department of Earth and Environmental Sciences, Ludwig-Maximilians-Universität, Theresienstr. 41, 80333 Munich, Germany
e-mail: hadzii@geophysik.uni-muenchen.de

P. Gaebler
Helmholtz-Zentrum Potsdam, Deutsches GeoForschungsZentrum GFZ, Sektion 2.4 Seismologie, Telegrafenberg, 14473 Potsdam, Germany

U. Schreiber
Forschungseinrichtung Satellitengeodäsie, Fundamental Station Wettzell, Sackenrieder Strasse 25, 93444 Bad Kötzting, Germany

1 Introduction

To fully describe the seismic wave field, one needs to measure three components of translational motion, six components of strain, and three components of rotational motion (Aki and Richards 2002). The use of seismometers and strainmeters to measure translational motion and strain, respectively, has been established for decades (e.g. Alsop et al. 1961; Gomberg and Agnew 1996). On the other hand, instruments suitable for measuring rotational motions are only starting to make their appearance. In particular, the development of high sensitivity ring laser gyroscopes has made it possible to detect rotational motions excited by seismic events (Stedman et al. 1995; McLeod et al. 1998; Pancha et al. 2000).

One interesting property is that, assuming plane wave propagation, the amplitude ratio of rotational motion around a vertical axis and the transverse acceleration is twice the horizontal phase velocity (Pancha et al. 2000; Igel et al. 2005;

Published online: 03 March 2012

Ferreira and Igel 2009). Kurrle et al. (2010) have shown the possibility and associated difficulties of determining local Love wave dispersion curves using such colocated measurement of both types of ground motion resulting from several seismic events. Igel et al. (2007) used the same method to determine the back azimuth of a seismic event as well. This paper concentrates on the application of the method to ambient noise. We study the origin of oceanic noise sources using two methods: amplitude ratios of colocated measurements of translational and rotational motions recorded at Wettzell, Germany (Schreiber et al. 2009), and classical $f-k$ analysis using the Gräfenberg array.

Previously, McLeod et al. (1998) and Pancha et al. (2000) have shown that ring laser gyroscopes provide sufficient accuracy to measure seismically induced ground rotations. However, for this study, it is important to determine if the Wettzell ring laser is sufficiently sensitive to continually detect ambient seismic noise. In Section 2, we characterize the noise level of the Wettzell ring laser. Sections 3 and 4 detail the theory and processing applied, respectively. In Section 5, we determine the noise source direction using only colocated rotational and translational measurements, for two different time periods. The reliability of these results is then assessed using independent array analysis in Section 6.

2 Characterization of noise on Wettzell ring laser

Most ambient noise in the periods from 5 to 20 s is generated by the interaction of the atmosphere, ocean waves, and the ground. The spectrum of this oceanic noise is dominated by two peaks, the primary microseismic peak at a period around 14 s and the secondary microseismic peak around 7 s (e.g. Friedrich et al. 1998). Longuet-Higgins (1950) suggests that the primary microseismic peak originates directly from forces on the seafloor induced by strong oceanic waves. The stronger secondary microseisms are believed to result from nonlinear interaction of these waves, producing the double-frequency peak. In both cases, the microseismic noise is dominated by fundamental mode surface waves, with Rayleigh waves contributing four times as much energy as Love waves in the secondary microseismic band (Friedrich et al. 1998).

Numerous past studies have attempted to localize the origin of primary and secondary microseisms (e.g. Gutenberg 1947; Cessaro 1994; Landès et al. 2010). In this study, we attempt to determine the back azimuthal direction of the strongest microseismic source using colocated rotational motion and transverse acceleration measurements.

This study uses rotational motions recorded at the ring laser of the Wettzell Geodetic Observatory in Germany (see Fig. 1). Ring lasers are active interferometers, where a polygon cavity is used in both directions to generate a spectrally narrow laser beam. Depending on the experienced rotation by the entire apparatus, these two counter-propagating laser beams differ slightly in optical frequency. Beating the two light beams against each other yields an interferogram, which

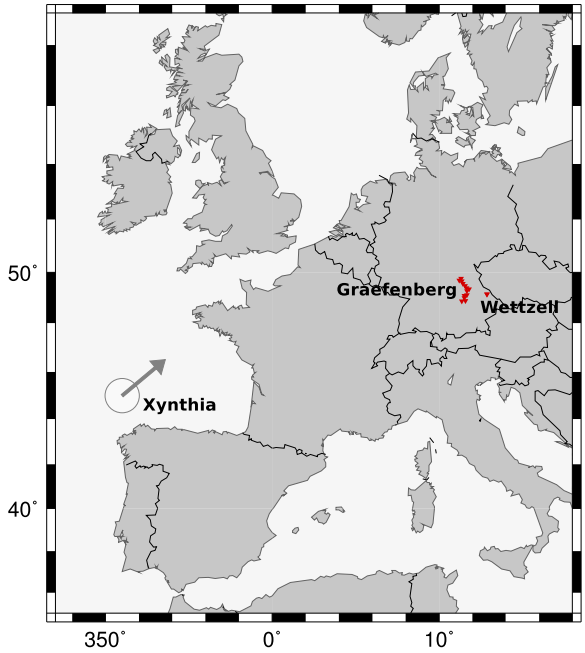

Fig. 1 Location of Gräfenberg seismic array and the Wettzell Geodetic Observatory. Stations WET and RLAS are located at the latter. The location of the Xynthia storm on February 27, 2010 as well as its direction are indicated by the *circle* and *arrow* (see also Section 5)

is strictly proportional to the experienced rate of rotation. The lower the loss of the mirrors, the smaller is the linewidth of the laser function and consequently, the higher the resolution of the sensor. In 2009, the ring laser was upgraded with fused silica mirrors for which a superior polish can be achieved, which improved the gyroscope performance.

To establish if oceanic microseisms can be detected with this instrument, its overall noise level is studied first. We characterize the noise recorded on the Wettzell ring laser (RLAS) using the method described in McNamara and Buland (2004). In this method, a statistical analysis is performed on power spectral densities taken at 1-h segments of noise. The analysis yields the probability density function of the noise power as a function of frequency for each station component.

In order to compare the noise level before and after the instrument improvement in 2009, 2 months of continuous recordings in the quiet summer periods of 2008 and 2010 were used. The top curve in Fig. 2 represents the background noise power before the mirror upgrade; the bottom curve represents the same afterwards. The flat behavior of the top curve is in agreement with the results by Widmer-Schnidrig and Zürn (2009) and is most likely due to instrument noise, not ambient seismic noise.

Figure 2 shows that the overall instrument noise level on the Wettzell ring laser decreased by 20 dB after the instrument upgrade, which corresponds to a factor 10 in amplitude. After 2009 (bottom curve), an elevated noise level with respect to the mostly flat instrument noise is visible in the 0.1–0.2 Hz range demonstrating that the Wettzell ring laser is capable of detecting ambient noise in the secondary microseismic peak. The detection of ambient noise in the primary microseismic peak (0.05–0.1 Hz) is more ambiguous. The reasons for this different detection level are the significantly higher amplitudes excited by the secondary microseisms in comparison to the primary microseisms, making the first easier to observe (Berger et al. 2004).

Since we have established that the Wettzell ring laser detects the secondary microseisms, the analysis in the next sections will concentrate on the corresponding frequency band (0.1–0.2 Hz).

3 Theory

For a horizontally polarized plane wave propagating in a homogeneous medium, the similarity

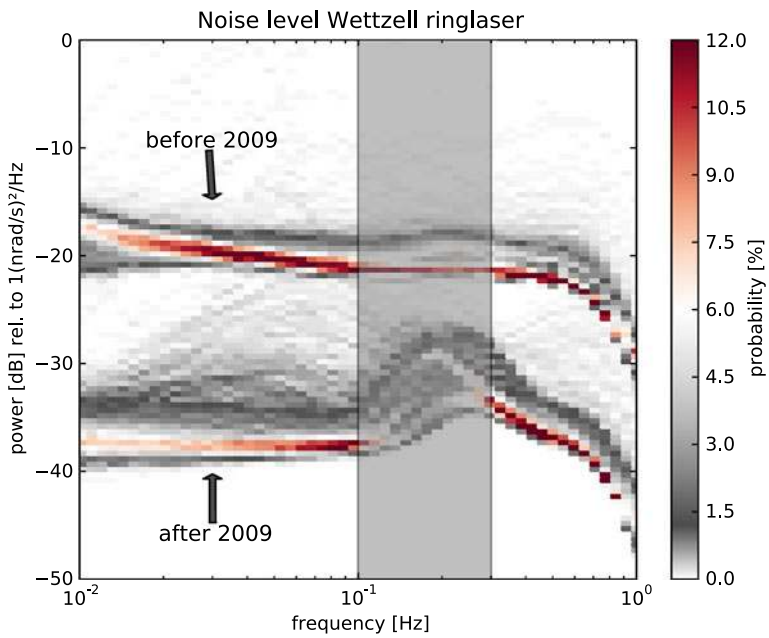

Fig. 2 Wettzell ring laser noise level relative to 1 $(\text{nrad/s})^2/\text{Hz}$ *before* (*top curve*) and *after* (*bottom curve*) an instrument improvement in 2009 (after McNamara and Buland 2004). Noise levels determined during the summer months of 2008 and 2010, respectively. The color scale indicates the probability of measuring a certain noise level, the *gray shading* corresponds to the secondary microseismic band

between colocated measurements of vertical rotation rate ($\dot{\omega}_z$) and transverse acceleration (a_T) is expected to be maximal. The displacement field for an incident wave, transversely polarized along the y-axis, is defined as follows:

$$\mathrm{u} = [0,\, A\sin(kx - kct),\, 0] \tag{1}$$

with amplitude A, wave number k, phase velocity c, and radial frequency ω. The displacement field $\mathbf{u}$ and rotational motions ω are related by the following:

$$\omega = \begin{pmatrix} \omega_x \\ \omega_y \\ \omega_z \end{pmatrix} = \frac{1}{2}\nabla \times \mathrm{u} = \frac{1}{2}\begin{pmatrix} \partial_y u_z - \partial_z u_y \\ \partial_z u_x - \partial_x u_z \\ \partial_x u_y - \partial_y u_x \end{pmatrix} \tag{2}$$

The rotation rate around a vertical axis $\dot{\omega}_z$ is then given by the following:

$$\dot{\omega}_z = \frac{1}{2}k^2 cA\sin(kx - kct), \tag{3}$$

while the transverse acceleration is given by the following:

$$a_T = \ddot{u}_T = -k^2c^2A\sin(kx - kct). \tag{4}$$

From Eqs. 3 and 4, the ratio between the transverse acceleration and the vertical rotation rate is as follows:

$$\frac{a_T}{\dot{\omega}_z} = \frac{-k^2c^2A\sin(kx - kct)}{\frac{1}{2}k^2cA\sin(kx - kct)} = -2c \tag{5}$$

This simple relation means that we can estimate phase velocities from the amplitude ratio of colocated measurements of rotational and translational motions.

From Eq. 5, we can also see that the two signals should have the same waveform, save for the $-2c$ factor. This property can be used to estimate the source direction of SH-type motions by rotating the horizontal components of the seismometer record along different angles, until their resemblance with the rotational measurements is maximal. The corresponding angle will then point in the direction of the source. Igel et al. (2007) and Kurrle et al. (2010) have applied this analysis to seismic events. In the next section, it will be applied to ambient noise in the secondary microseismic band.

4 Processing

The rotational motion around the vertical axis ($\dot{\omega}_z$) is measured with the RLAS, while the translational ground motion is measured with a STS2 broadband seismometer at the German Regional Seismic Network station WET (see Fig. 1). This seismometer is located less than 260 m from the ring laser and can thus be considered as colocated with the ring laser for the frequency range investigated in this study.

The seismometer velocity records are corrected for instrument response and differentiated to obtain the acceleration. The records from the ring laser only need to be divided by a frequency-independent gain factor to obtain the rotation rate. Finally, all signals are bandpass-filtered using a fourth-order Butterworth filter in the secondary microseismic band at 0.1–0.2 Hz. All processing is done with the ObsPy toolbox (Beyreuther et al. 2010; Megies et al. 2011).

According to Eq. 5, the amplitude ratio of transverse acceleration and vertical rotation rate gives the apparent phase velocity. The back azimuth of the source can also be determined by rotating the horizontal components of the transverse acceleration until the similarity with the vertical rotation rate signal is maximal.

First, a back azimuth vector is defined with evenly distributed angles between 0° and 360°. The transversal acceleration a_T is then obtained for each back azimuth angle θ_i by rotating the horizontal acceleration components. The similarity between the transversal acceleration and the rotation rate is quantified by calculating the cross-correlation coefficient, which is defined between 0 for no similarity and 1 for a perfect match. The back azimuth angle for the best-fitting transverse acceleration points in the direction of the source.

This process is repeated for a number of overlapping, moving time windows along the signal in order to follow the evolution of the main source orientation. The time window length is fixed at the central period T_c a few times. For each 60-s window, for which the cross-correlation coefficient

between the two signals exceeds a threshold which we set at 0.75, the phase velocity is estimated according to Eq. 5. This is done by finding the optimal scaling between the rotation rate and the best-fitting transverse acceleration, according to a least squares method.

In the following section, this procedure is tested on a seismic event with known back azimuth, as well as on a day with a strong microseismic source.

5 Results

First of all, the amplitude ratio method is tested on a seismic event, using two frequency bands: the first excluding oceanic microseisms (0.01–0.03 Hz, Fig. 3) and the second centered on the secondary microseismic peak (0.1–0.2 Hz, Fig. 4). On March 11, 2011 the M_W9.0 Tohoku-Oki event occurred at 05:46 UTC, with a theoretical back azimuth of 37° relative to the Wettzell station. Figures 3b and 4b show the cross-correlation coefficient between rotational and transverse measurements as a function of back azimuth and time. In Fig. 3, with the microseismic frequency bands excluded, the waveform cross-correlation exceeds the threshold value of 0.75 only at the times of the main event and subsequent aftershocks. The correlation coefficient at those times reaches a maximum at the theoretical back azimuth of the event (red

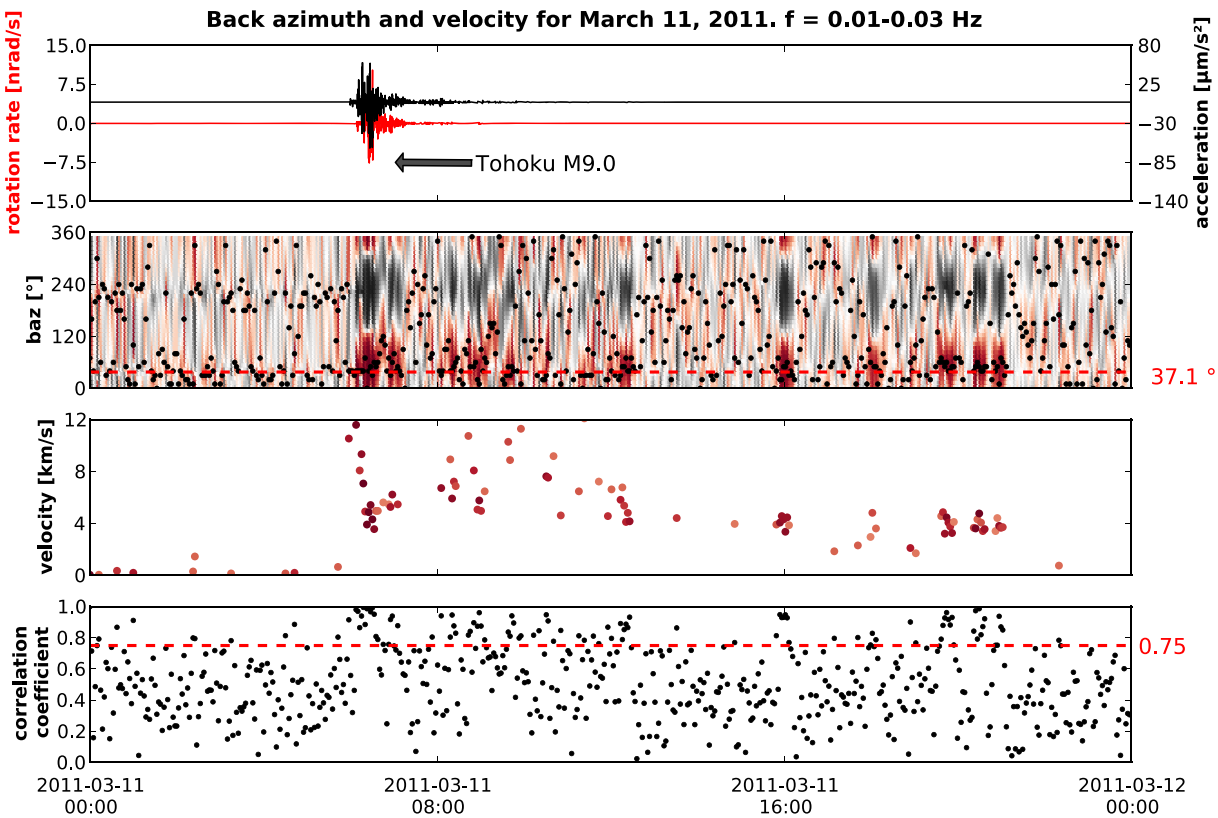

Fig. 3 Data for March 11, 2011, with the M_W9.0 Tohoku-Oki event at a back azimuth of 37°. **a** Traces for rotation rate in *red* and transverse acceleration in *black*. **b** Back azimuth, with color scale indicating the cross-correlation coefficient for each back azimuth, where *red* is a positive high and *black* a negative high. A *black dot* marks the maximum correlation coefficient. The theoretical back azimuth of the Tohoku-Oki event dashed by a *red* line. **c** Phase velocity obtained from amplitude ratio ($\frac{a_T}{\omega_z}$), color scale corresponds to the correlation coefficient as in **b**. **d** Maximum correlation coefficient between rotation rate and transverse acceleration. The *red dashed line* indicates the threshold value of 0.75. Frequency band f = 0.01–0.03 Hz excludes the secondary microseismic peak

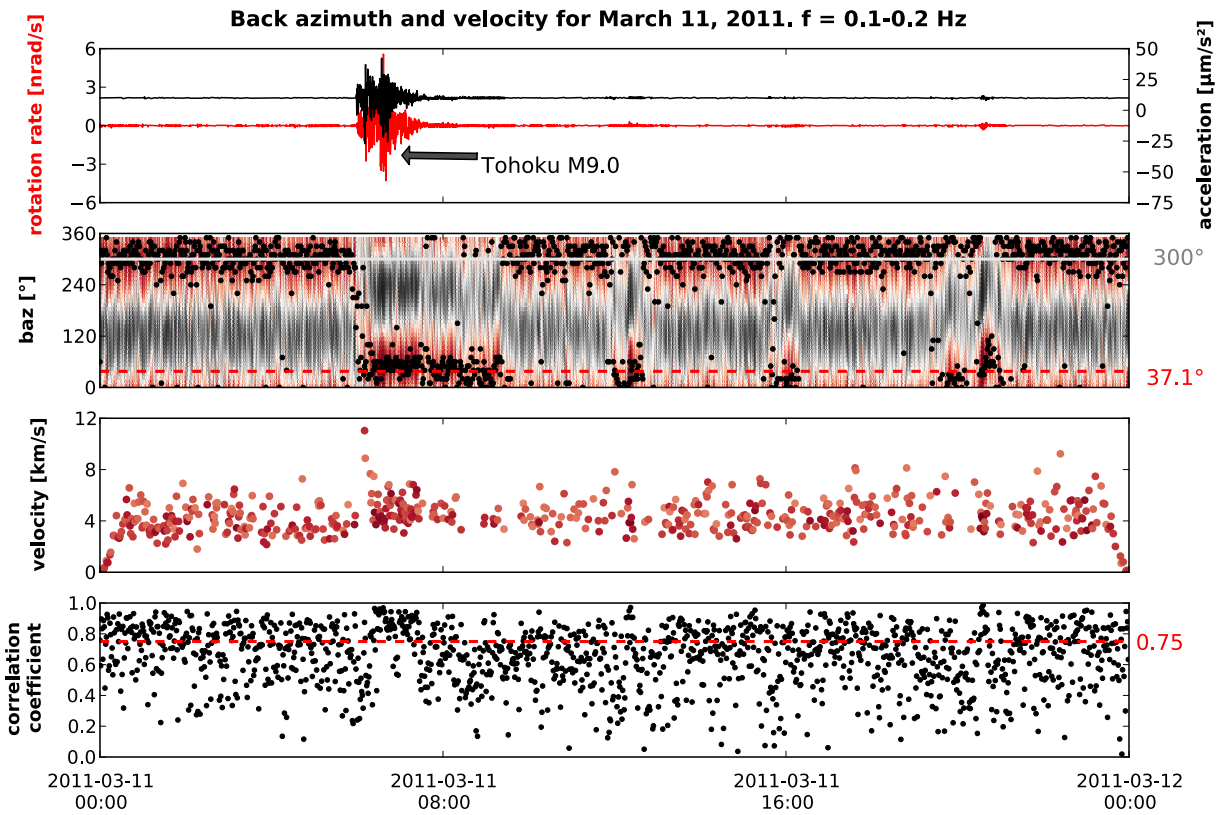

Fig. 4 As in Fig. 3, but at f = 0.1–0.2 Hz, including the secondary microseismic peak

dashed line), which indicates that the method works for seismic events. The apparent phase velocities attain realistic values as well of the order of 12 km/s for a steep incidenting S wave arrival, then dropping to values around 4 km/s, which corresponds well to theoretical Love wave phase velocities.

When the frequency band is centered on the secondary microseismic peak (Fig. 4), the waveform correlation stays high throughout the day, even in an absence of any seismic events. At times without seismic events, the maximum of the correlation coefficient consistently lies at a back azimuth of 300°. This suggests that we are observing a microseismic noise source with a back azimuth of 300°. This observation is supported by the work of Darbyshire (1991) and Friedrich et al. (1998), who both find a source of secondary microseismic noise in the Channel region.

The results from using data with a major seismic event are promising and even seem to show a consistent microseismic source. To test if ambient noise source directions can be found, the method is tested on a time period with a strong acting source of oceanic noise at a known location. On February 26, 2010, the Xynthia storm originated 30° off the west coast of Portugal (see Fig. 1). A high energy low pressure system like the Xynthia storm significantly increases the height of ocean waves while it is on the open sea or near coastlines. Such increased wave height is directly linked to the generation of primary and secondary microseismic noise. This particular storm generated strong microseismic activity at a back azimuth of around 260° with respect to Wettzell. In addition to this, on the same date, a seismic event occurred in Japan (M_W7.0 Ryukyu event) with a theoretical back azimuth of around 45°.

Figure 5 shows the signals for vertical rotation rate and transverse acceleration, the apparent phase velocity obtained using amplitude ratios, the cross-correlation coefficient for each

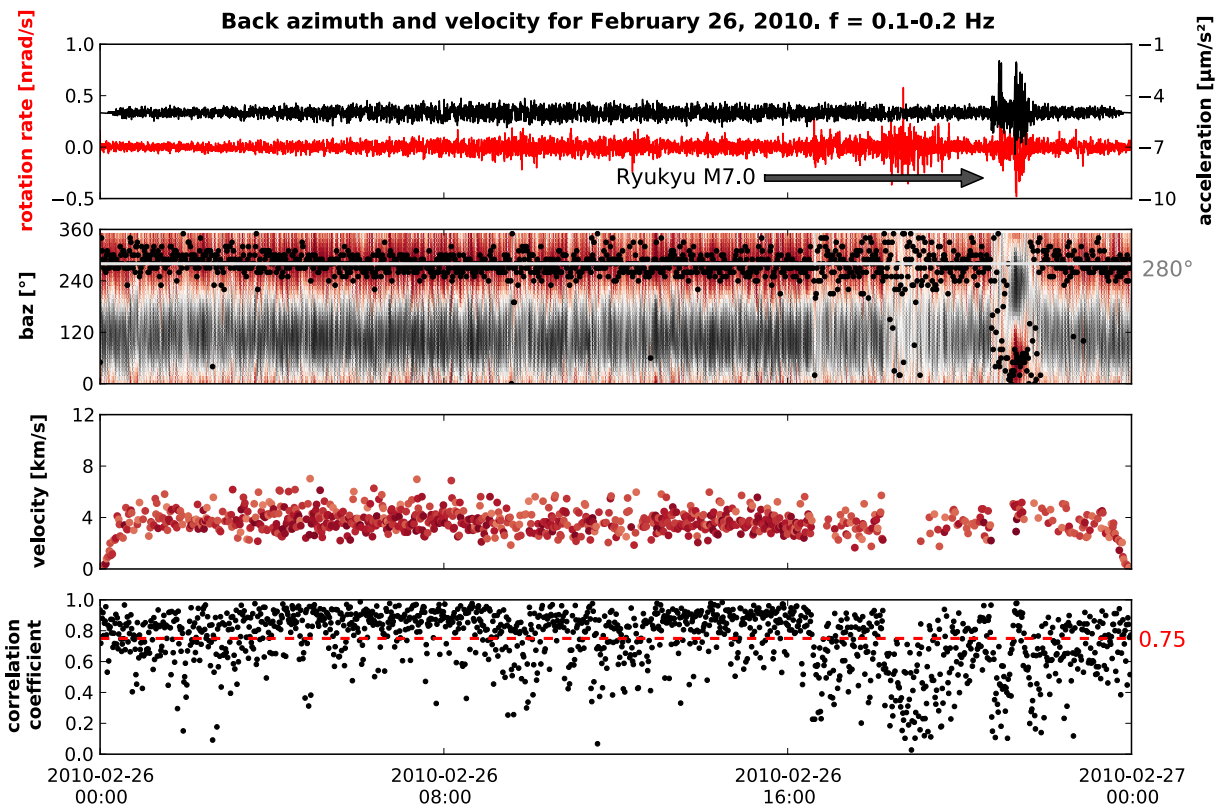

Fig. 5 One-day data during the Xynthia storm (February 26, 2010). Event is the M_W7.0 Ryukyu event with a back azimuth of 45°. **a** Traces for rotation rate in *red* and transverse acceleration in *black*. **b** Back azimuth, with color scale indicating the cross-correlation coefficient for each back azimuth, where *red* is positive high and *black* negative high. A *black dot marks* the maximum correlation coefficient. Median back azimuth is indicated by a *white line*. **c** Phase velocity obtained from amplitude ratio ($\frac{a_T}{\omega_z}$), color scale corresponds to the correlation coefficient as in **b**. **d** Maximum correlation coefficient between rotation rate and transverse acceleration. The *red dashed line* indicates the threshold value of 0.75. f = 0.1–0.2 Hz

back azimuth as a color scale, and finally the maximum correlation coefficient. Over the course of the day, a maximum cross-correlation coefficient (fluctuating around 0.8) is found at a back azimuth of ∼ 270°. This corresponds roughly to the southwestern direction and matches the expected back azimuth of the Xynthia storm (260°) closely. In addition to this, the correlation coefficient briefly reaches a maximum value for a back azimuth of ∼ 50° at the time of the Ryuku event.

Note the higher amplitudes of the ring laser measurement starting around 17:00 UTC. These fluctuations correlate with high wind speeds measured at the meteorological station in Wettzell. There are two possible phenomena at work here. First, strong wind gusts may cause a tilting effect on the ring laser system, which in turn can affect the measured rotation rate. However, Pham et al. (2009) showed that this effect is negligible in the case of strong teleseismic events and therefore is likely very small in the case of wind influence as well. A second cause can be modeled by shear forces on the building excited by strong local acting wind. These shear forces may be transmitted to the ring laser system and thus cause significant variations in the measured rotation rate. This sensitivity of the Wettzell ring laser to local wind speeds does not affect the results in this study, as the consequent decrease of cross-correlation coefficient disqualifies the affected time windows. However, it is important to be aware of this effect.

The results in this section give strong evidence that it is possible to find the direction and apparent phase velocity not only of seismic events but also of ambient noise sources as well, using only a point measurement. In the next section, we confirm the observations with an independent analysis using classic array processing methods.

6 Comparison to $f-k$ analysis

Following the promising results in the previous section, a frequency–wavenumber analysis is performed using data from the Gräfenberg seismic array (see Fig. 1) for both time periods analyzed in Section 5. This array consists of 13 three component broadband stations and is located about 50 km west of the Wettzell station (see Fig. 1). The aperture of the array and the average interstation distance make it suitable to study the microseismic band. Since the array is close to the Wettzell station, we can assume that the same noise sources are observed at both locations. Sources of ambient noise Rayleigh waves are believed to be at approximately the same locations as those of Love waves (Nishida et al. 2008). Therefore, only vertical component records are used in the array analysis.

The data from the Gräfenberg stations are corrected for instrument response, and bandpass-filtered for 0.1–0.2 Hz using a fourth order Butterworth filter. Next, frequency–wavenumber

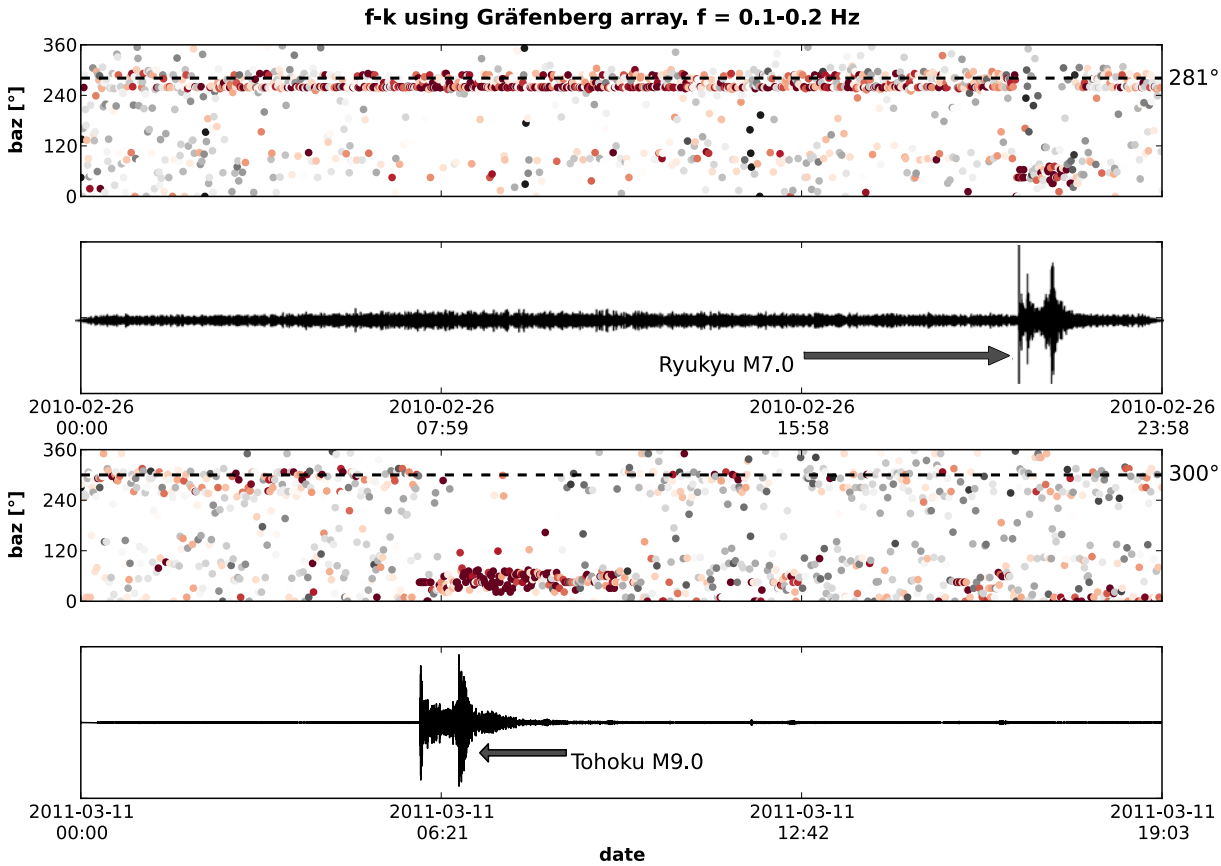

Fig. 6 Frequency–wavenumber analysis on the Z-component of the Gräfenberg array. *Top*: during the Xynthia storm (February 26, 2010). Event is the M_W7.0 Ryukyu event. *Bottom*: during the M_W9.0 Tohoku-Oki event (March 11, 2011). Back azimuth value obtained for microseismic signal with the amplitude ratio ($\frac{a_T}{\omega_z}$) indicated by a *dashed black line*, color scale indicates the beam power with *red high* and *black low*. Signals are recorded at station GRA1. f = 0.1-0.2 Hz

analysis is performed for a moving time window. The length of the time window is taken such that more than one wavelength of the slowest waves is recorded over the whole array. The beampower maximum is picked for each time window, and its back azimuth is represented in Fig. 6. The back azimuths found using the amplitude ratio method described in Section 3 are indicated in the figures as a black dashed line. At both dates, consistent noise sources are detected at back azimuths of 270°–280°, respectively. As in Fig. 4, the back azimuth found in Fig. 6 temporarily shifts to the direction of the Tohoku-Oki event and its aftershocks.

The excellent agreement with the results from classic frequency–waveform analysis proves that it is possible to determine the ambient noise source orientation using only a colocated measurement of rotation rate and transverse acceleration.

7 Discussion and conclusion

Recently, improved sensitivity of sensors have made it possible to observe rotational ground motions induced by seismic events. However, the consistent observation of rotational motions in ambient noise has proven difficult. We have shown that, as a result of the instrument improvement in 2009, the Wettzell ring laser can detect rotational motions in microseisms in the secondary microseismic band (0.1–0.2 Hz).

A colocated measurement of rotation rate and transverse acceleration lead to a back azimuth estimation as well as one for the apparent phase velocity. By applying the method detailed in Section 3, a consistent high correlation between rotation rate and transverse acceleration signals is found in the secondary microseismic band, which is not present at other frequencies. This high correlation points to a noise source at a back azimuth of 300°. Testing the same method with a different data set including a date with a strong noise source (the Xynthia storm) yields a back azimuth close to the theoretical value of ∼260°. The apparent velocities found with this method correspond to the expected local values.

Finally, these results are checked against classic array beamforming analysis. For practical reasons, this $f-k$ analysis was performed on vertical component records and thus using mainly Rayleigh waves. However, since both ambient noise Rayleigh and Love waves are believed to be generated in the same areas (Nishida et al. 2008), the results can still be compared. Using array beamforming techniques, the same main source back azimuths are found as with the amplitude ratio method in Section 5.

We have shown that measurements of rotational and translational motions in ambient noise at a single location can be used to make observations consistent with traditional methods which require arrays of translational instruments. However, currently, only very expensive instruments such as the Wettzell ring laser are sensitive enough to detect the rotational motions in ambient noise. This illustrates the importance of developing less expensive rotational sensors with low noise levels.

Acknowledgements We gratefully acknowledge the support from the European Commission (Marie Curie Actions, ITN QUEST, www.quest-itn.org) and the German Research Foundation (project Ig16-8).

References

Aki K, Richards P (2002) Quantitative seismology. Second edition, University Science Books, Sausalito, California

Alsop L, Sutton G, Ewing M (1961) Free oscillations of the Earth observed on strain and pendulum seismographs. J Geophys Res 66(2):631–641

Berger J, Davis P, Ekström G (2004) Ambient Earth noise: a survey of the global seismographic network. Geophys Res Lett 109:B11,307

Beyreuther M, Barsch R, Krischer L, Megies T, Behr Y, Wassermann J (2010) Obspy: a Python toolbox for seismology. Seismol Res Lett 81(3):530–533

Cessaro R (1994) Sources of primary and secondary microseisms. Bull Seismol Soc Am 84(1):142

Darbyshire J (1991) A further investigation of microseisms recorded in North Wales. Phys Earth Planet Inter 67(3–4):330–347

Ferreira A, Igel H (2009) Rotational motions of seismic surface waves in a laterally heterogeneous Earth. Bull Seismol Soc Am 99(2B):1429

Friedrich A, Krüger F, Klinge K (1998) Ocean-generated microseismic noise located with the Gräfenberg array. J Seismol 2(1):47–64

Gomberg J, Agnew D (1996) The accuracy of seismic estimates of dynamic strains: an evaluation using strain-

meter and seismometer data from Pinon Flat Observatory, California. Bull Seismol Soc Am 86(1A):212
Gutenberg B (1947) Microseisms and weather forcecasting. Journal of Meteorology 4(1):21–28
Igel H, Schreiber U, Flaws A, Schuberth B, Velikoseltsev A, Cochard A (2005) Rotational motions induced by the M8.1 Tokachi-Oki earthquake, September 25, 2003. Geophys Res Lett 32:L08,309
Igel H, Cochard A, Wassermann J, Flaws A, Schreiber U, Velikoseltsev A, Pham Dinh N (2007) Broad-band observations of earthquake-induced rotational ground motions. Geophys J Int 168(1):182–196
Kurrle D, Igel H, Ferreira AMG, Wassermann J, Schreiber U (2010) Can we estimate local Love wave dispersion properties from collocated amplitude measurements of translations and rotations? Geophys Res Lett 37(4):1–5
Landès M, Hubans F, Shapiro NM, Paul A, Campillo M (2010) Origin of deep ocean microseisms by using teleseismic body waves. J Geophys Res 115(B5): 1–14
Longuet-Higgins M (1950) A theory of the origin of microseisms. Philos Trans R Soc Lond Ser A: Math Phys Sci 243(857):1–35
McLeod D, Stedman G, Webb T, Schreiber U (1998) Comparison of standard and ring laser rotational seismograms. Bull Seismol Soc Am 88(6):1495
McNamara DE, Buland RP (2004) Ambient noise levels in the continental United States. Bull Seismol Soc Am 94(4):1517–1527
Megies T, Beyreuther M, Barsch R, Krischer L, Wassermann J (2011) Obspy–what can it do for data centers and observatories? Ann Geophys 54(1):47–58
Nishida K, Kawakatsu H, Fukao Y, Obara K (2008) Background Love and Rayleigh waves simultaneously generated at the Pacific Ocean floors. Geophys Res Lett 35(16):1–5
Pancha A, Webb TH, Stedman GE, McLeod DP, Schreiber KU (2000) Ring laser detection of rotations from teleseismic waves. Geophys Res Lett 27(21):3553
Pham N, Igel H, Wassermann J, Kaser M, de La Puente J, Schreiber U (2009) Observations and modeling of rotational signals in the P-coda: constraints on crustal scattering. Bull Seismol Soc Am 99(2B):1315
Schreiber K, Hautmann J, Velikoseltsev A, Wassermann J, Igel H, Otero J, Vernon F, Wells J (2009) Ring laser measurements of ground rotations for seismology. Bull Seismol Soc Am 99(2B):1190
Stedman G, Li Z, Bilger H (1995) Sideband analysis and seismic detection in a large ring laser. Appl Opt 34(24):5375–5385
Widmer-Schnidrig R, Zürn W (2009) Perspectives for ring laser gyroscopes in low-frequency seismology. Bull Seismol Soc Am 99(2B):1199